Langmuir
The ACS Journal of Surfaces and Colloids

JANUARY 17, 2006
VOLUME 22, NUMBER 2

# *Letters*

## Characterization of Micro-Mesoporous Materials from Nitrogen and Toluene Adsorption: Experiment and Modeling

Peter I. Ravikovitch,*,† Aleksey Vishnyakov,† Alexander V. Neimark,*,†
Manuela M. L. Ribeiro Carrott,‡ Patrícia A. Russo,‡ and Peter J. Carrott‡

*Center for Modeling and Characterization of Nanoporous Materials, TRI/Princeton, 601 Prospect Ave., Princeton, New Jersey 08540 USA, and Centro de Química de Évora and Departamento de Química, Universidade de Évora, Colégio L. A. Verney, 7000-671 Évora, Portugal*

*Received August 12, 2005. In Final Form: October 4, 2005*

Universal mechanisms of adsorption and capillary condensation of toluene and nitrogen on ordered MCM-41 and PHTS materials are studied by means of high-resolution experiments and Monte Carlo molecular simulations. A molecular simulation model of toluene adsorption in silica nanopores, which accounts for surface heterogeneity, and a hybrid molecular-macsroscopic method for pore size distribution (PSD) calculations have been developed. For a range of reference materials, the PSD results obtained from toluene isotherms are consistent with the results of nitrogen adsorption using the nonlocal density functional theory method.

### Introduction

The emergence of ordered adsorbents, such as MCM-41,[1] SBA-15,[2] and related materials,[3] has catalyzed experimental,[4−9] theoretical,[5,10−12] and simulation[10,13−16] studies of adsorption in pores of well-defined geometries, and made possible the development of new molecular-based methods for pore size distribution (PSD) analysis (see ref 17 for a recent review). Methods of nonlocal density functional theory (NLDFT) have been developed for $N_2$ and Ar PSD characterization of siliceous mesoporous materials with cylindrical[18] and spherical[11] pores, as well as micro-mesoporous materials.[19,20] At the nanometer

* To whom correspondence should be addressed. E-mail: ravikovi@triprinceton.org (P.I.R.); aneimark@triprinceton.org (A.V.N.).
† TRI/Princeton.
‡ Universidade de Évora.

(1) Beck, J. S.; Vartuli, J. C.; Roth, W. J.; Leonowicz, M. E.; Kresge, C. T.; Schmitt, K. D.; Chu, C. T. W.; Olson, D. H.; Sheppard, E. W.; McCullen, S. B.; Higgins, J. B.; Schlenker, J. L. *J. Am. Chem. Soc.* **1992**, *114*, 10834−10843.
(2) Zhao, D. Y.; Feng, J. L.; Huo, Q. S.; Melosh, N.; Fredrickson, G. H.; Chmelka, B. F.; Stucky, G. D. *Science* **1998**, *279*, 548−552.
(3) Zhao, D. Y.; Huo, Q. S.; Feng, J. L.; Chmelka, B. F.; Stucky, G. D. *J. Am. Chem. Soc.* **1998**, *120*, 6024−6036.
(4) Branton, P. J.; Hall, P. G.; Sing, K. S. W.; Reichert, H.; Schuth, F.; Unger, K. K. *J. Chem. Soc.-Faraday Trans.* **1994**, *90*, 2965−2967.
(5) Ravikovitch, P. I.; O'Domhnaill, S. C.; Neimark, A. V.; Schuth, F.; Unger, K. K. *Langmuir* **1995**, *11*, 4765−4772.
(6) Kruk, M.; Jaroniec, M.; Sayari, A. *J. Phys. Chem. B* **1997**, *101*, 583−589.
(7) Morishige, K.; Shikimi, M. *J. Chem. Phys.* **1998**, *108*, 7821−7824.
(8) Ribeiro Carrott, M. M. L.; Candeias, A. J. E.; Carrott, P. J. M.; Ravikovitch, P. I.; Neimark, A. V.; Sequeira, A. D. *Microporous Mesoporous Mater.* **2001**, *47*, 323−337.
(9) Ravikovitch, P. I.; Neimark, A. V. *Langmuir* **2002**, *18*, 9830−9837.
(10) Neimark, A. V.; Ravikovitch, P. I.; Vishnyakov, A. *Phys. Rev. E* **2000**, *62*, R1493−R1496.
(11) Ravikovitch, P. I.; Neimark, A. V. *Langmuir* **2002**, *18*, 1550−1560.
(12) Ustinov, E. A.; Do, D. D.; Jaroniec, M. *J. Phys. Chem. B* **2005**, *109*, 1947−1958.
(13) Maddox, M. W.; Olivier, J. P.; Gubbins, K. E. *Langmuir* **1997**, *13*, 1737−1745.
(14) Neimark, A. V.; Vishnyakov, A. *Phys. Rev. E* **2000**, *62*, 4611−4622.
(15) He, Y. F.; Seaton, N. A. *Langmuir* **2003**, *19*, 10132−10138.
(16) Kuchta, B.; Llewellyn, P.; Denoyel, R.; Firlej, L. *Low Temp. Phys.* **2003**, *29*, 880−882.
(17) Thommes, M. In *Nanoporous Materials: Science and Engineering*; Lu, M., Zhao, G., Eds.; Imperial College Press: London, 2004; Vol. Chapter 11, p 317.
(18) Ravikovitch, P. I.; Wei, D.; Chueh, W. T.; Haller, G. L.; Neimark, A. V. *J. Phys. Chem. B* **1997**, *101*, 3671−3679.
(19) Ravikovitch, P. I.; Neimark, A. V. *J. Phys. Chem. B* **2001**, *105*, 6817−6823.
(20) Smarsly, B.; Thommes, M.; Ravikovitch, P. I.; Neimark, A. V. *Adsorption* **2005**, *11*, 653−655.

10.1021/la052202k CCC: $33.50 
Published on Web 11/16/2005

**Table 1. Pore Structure Parameters of Mesoporous Silicas Determined from $N_2$ Adsorption Isotherms Using the NLDFT Method and Toluene Adsorption Isotherms Using the Developed Hybrid MC-DBdB Method**

| sample | $N_2$ pore diameter, nm | toluene pore diameter, nm | $N_2$ pore volume, $cm^3/g$ | toluene pore volume, $cm^3/g$ |
|---|---|---|---|---|
| MCM-41 (C14)[a] | 3.2 | 3.3 | 0.67[d] | 0.62[d] |
| MCM-41 (C16)[a] | 3.8 | 3.9 | 0.80[d] | 0.73[d] |
| MCM-41 (C50)[b] | 4.5 | 4.5 | 0.63[d] | 0.61[d] |
| PHTS[c] | 7.3 (1−2)[e] | 7.3 (1.2−2)[e] | 0.64[d] (0.15) [f] | 0.59[d] (0.1) [f] |

[a] Prepared as described in ref 8. [b] Sample described in ref 5. [c] Sample similar to materials described in ref 28. [d] Volume of pores below 10 nm. [e] Micropore size. [f] Micropore volume.

scale, the NLDFT methods significantly improve the accuracy of $N_2$ and Ar adsorption porosimetry over macroscopic Kelvin equation based methods.[5,21]

This work is motivated by the necessity of developing adequate methods for PSD characterization of low-k dielectric films. Low-k films with nanoscale porosity are of great importance to the semiconductor industry.[22,23] However, the standard methods of $N_2$ and Ar porosimetry do not provide enough sensitivity to measure adsorption in thin films.[23−25] Ellipsometric[24] and X-ray reflectivity[25−27] techniques have been developed to assess adsorption/desorption isotherms of organic vapors in thin films. Traditionally, toluene is used in these techniques as an adsorbate. However, a quantitative interpretation of toluene adsorption/desorption isotherms in terms of PSDs is challenging because of the well-known shortcomings of the macroscopic Kelvin equation based methods at the nanoscale. In addition, many low-k dielectric materials are microporous.

In this paper, we describe universal features of toluene and nitrogen adsorption and a method for calculating micro- and mesopore size distributions from toluene adsorption isotherms based on a combination of experimental measurements on ordered materials and molecular simulations.

## Materials and Methods

**Experimental.** In this work, we used MCM-41[5,8] and plugged hexagonal templated silica (PHTS)[28] materials consisting of a hexagonal array of cylindrical mesopores (see Table 1). In MCM-41, the mesopores are noninterconnected and the pore walls are similar to amorphous silicas. PHTS materials are related to SBA-15 materials synthesized by using nonionic surfactants. The pore walls are rough and microporous and, thus, permeable to small molecules. Some fraction of mesopores in PHTS contains constrictions or plugs. This creates a system of open (from one or both ends) and blocked (closed from both ends but permeable via microporous walls) cylindrical channels.

The adsorption/desorption isotherms of toluene at 298 K were determined gravimetrically using a CI Electronics MK2 vacuum microbalance with DISBAL control unit, with pressure measurement by means of Edwards Barocel 622 capacitance manometers. Nitrogen adsorption isotherms at 77 K were determined on Sorptomatic 1990 (CE Instruments) and Autosorb-1C (Quantachrome Instr.) automated volumetric instruments.

**Molecular Model of Toluene Adsorption.** Monte Carlo (MC) simulations of toluene adsorption were based on the united-atom model of Wick et al.[29] In this model, seven Lennard-Jones (LJ) interaction sites correspond to seven carbons of the toluene molecule, whereas hydrogens are accounted for implicitly (for details see the Supporting Information, Table S1). However, the LJ potential for fluid−fluid interactions was truncated at 0.97 nm. We checked by the gauge cell MC[30] simulations that this model reproduces well the saturated vapor pressure of toluene at 300 K (4.07 versus 4.17 kPa in experiment), but overpredicts the liquid density by 6% (0.91 $g/cm^3$ versus the experimental value of 0.86 $g/cm^3$).

The pores were modeled as infinite cylindrical channels with periodic boundary conditions. Solid−fluid interactions were represented by a LJ potential between each carbon atom of the toluene molecule and a structureless cylindrical layer of solid atoms, as described by Tjatjopoulos et al.[31] However, the structureless model of the solid was unable to describe adequately the experimental adsorption isotherm of toluene on MCM-41 at low pressures (see the Supporting Information, Figure S1). To account for surface heterogeneity of MCM-41, we roughened the fluid-solid energy landscape by placing additional attractive and repulsive sites randomly distributed over the surface (see the Supporting Information, Figure S2). Each site created a spherical potential well. If the center of mass of a toluene molecule was found within the well, a perturbation energy $\epsilon_{ww}$ of the order of 20% from the total solid−fluid energy of the molecule was added or subtracted (see Supporting Information for details).

Adsorption/desorption isotherms were simulated using the standard grand canonical MC (GCMC) method.[32] The pressure of the vapor−liquid equilibrium transition in mesopores was determined using the gauge cell simulation method[30] (see Supporting Information).

## Results and Discussion

**Universal Feature of Nitrogen and Toluene Adsorption.** Nitrogen and toluene isotherms on MCM-41 feature the region of mono- and multilayer adsorption followed by a sharp capillary condensation step (Figure 1). For the smaller pore diameter MCM-41 materials (C14 and C16), the step is completely reversible. As the pore diameter increases, a hysteresis loop develops, as seen for the MCM-41 C50 sample. The hysteresis loop is of type H1, according to IUPAC classification,[33] which corresponds to materials with open cylindrical pores. The curvature of the toluene isotherms on MCM-41 materials at low relative pressures (below $P/P_0 = 0.15$) is associated with a formation of adsorbed layers. PHTS material is microporous. Therefore, the curvature of the isotherm at low pressures is associated with adsorption in micropores and multilayer adsorption on the rough pore walls.

(21) Neimark, A. V.; Ravikovitch, P. I.; Vishnyakov, A. *J. Phys.-Condes. Matter* **2003**, *15*, 347−365.
(22) Morgen, M.; Ryan, E. T.; Zhao, J. H.; Hu, C.; Cho, T. H.; Ho, P. S. *Annu. Rev. Mater. Sci.* **2000**, *30*, 645−680.
(23) Maex, K.; Baklanov, M. R.; Shamiryan, D.; Iacopi, F.; Brongersma, S. H.; Yanovitskaya, Z. S. *J. Appl. Phys.* **2003**, *93*, 8793−8841.
(24) Baklanov, M. R.; Mogilnikov, K. P.; Polovinkin, V. G.; Dultsev, F. N. *J. Vac. Sci. Technol. B* **2000**, *18*, 1385−1391.
(25) Lee, H. J.; Soles, C. L.; Liu, D. W.; Bauer, B. J.; Wu, W. L. *J. Polym. Sci. Part B−Polym. Phys.* **2002**, *40*, 2170−2177.
(26) Lee, H. J.; Soles, C. L.; Liu, D. W.; Bauer, B. J.; Lin, E. K.; Wu, W. L. *J. Apll. Phys.* **2004**, *95*, 2355−2359.
(27) Soles, C. L.; Lee, H. J.; Lin, E. K.; Wu, W. L. *Pore Characterization in Low-k Dielectric Films Using X-ray Reflectivity: X-ray Porosimetry*; NIST Recommended Practice Guide: Gaithersburg, MD, 2004.
(28) Van Der Voort, P.; Ravikovitch, P. I.; De Jong, K. P.; Benjelloun, M.; Van Bavel, E.; Janssen, A. H.; Neimark, A. V.; Weckhuysen, B. M.; Vansant, E. F. *J. Phys. Chem. B* **2002**, *106*, 5873−5877.
(29) Wick, C. D.; Martin, M. G.; Siepmann, J. I. *J. Phys. Chem. B* **2000**, *104*, 8008−8016.
(30) Neimark, A. V.; Vishnyakov, A. *J. Chem. Phys.* **2005**, *122*.
(31) Tjatjopoulos, G. J.; Feke, D. L.; Mann, J. A. *J. Phys. Chem.* **1988**, *92*, 4006−4007.
(32) Allen, M. P.; Tildesley, D. J. *Computer Simulation of Liquids*; Clarendon Press: Oxford, U.K., 1987.
(33) Gregg, S. J.; Sing, K. S. W. *Adsorption, Surface Area and Porosity*; Academic Press: New York, 1982.

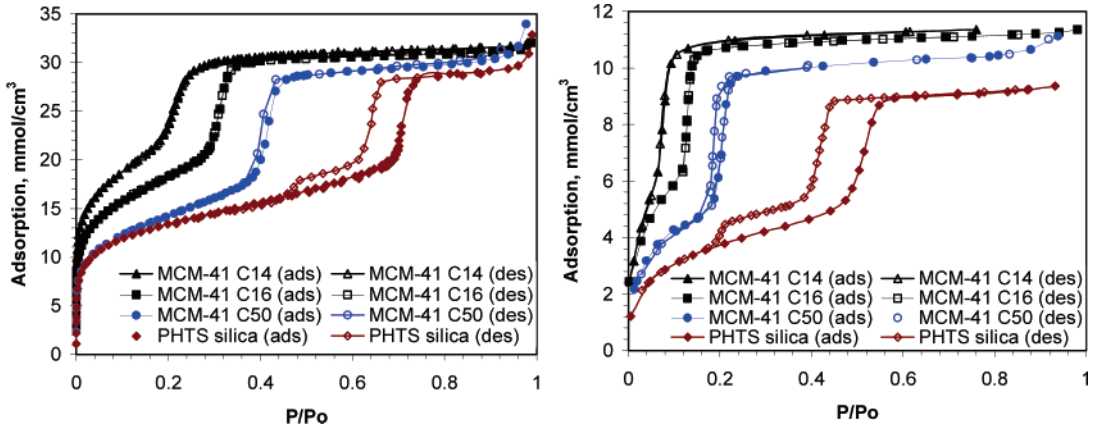


**Figure 1.** Nitrogen at 77 K (top) and toluene at 298 K (bottom) adsorption/desorption isotherms on reference silicas normalized by the total pore volume (see Table 1). For convenience, the vertical scale is shifted by 1, 2, and 3 mmol/cm$^3$ for samples MCM-41 C50, MCM-41 C16, and MCM-41 C14, respectively.

Similarly to MCM-41, nitrogen and toluene adsorption isotherms on PHTS exhibit a sharp capillary condensation step, indicating uniform pore size. Isotherms on PHTS exhibit a characteristic two-step desorption branch, which reflects two different mechanisms of desorption.[28] The first step (at a higher pressure) is associated with desorption from the open cylindrical channels. The second step is due to desorption from the blocked cylindrical channels. Desorption from the uniform open cylindrical pores is an equilibrium process, whereas desorption from the blocked pores depends on the size of constrictions. If constrictions are sufficiently wide, the desorption pressure is determined by the size of constrictions (classical ink-bottle or pore blocking effect). In the case of PHTS, the constrictions are narrow (below 4−5 nm), and desorption is triggered by cavitation in the metastable fluid. The pressure of cavitation does not reflect the size of the constrictions or the size of the pore itself.[9] For nitrogen in PHTS, cavitation occurs at the relative pressure of $P/P_0 = 0.45$, whereas for toluene it occurs at $P/P_0 = 0.2$. The mechanisms of toluene adsorption/desorption are in agreement with our recent theoretical,[11] experimental[9] and molecular simulation[34] studies of adsorption−desorption hysteresis of $N_2$, Ar, and Kr in materials with open and blocked pores. It is worth noticing that the adsorption/desorption isotherms of toluene on some porous low-k films, which contain relatively large voids, also exhibit a desorption step at $P/P_0 = 0.2$[35] that we attribute to cavitation.

**Comparison of Simulations with Experiment.** Snapshots of molecular configurations in a cylindrical pore of 4.5 nm in diameter show that toluene forms a disordered multilayer before capillary condensation transition (Figure 2, left). This behavior is a consequence of the heterogeneity introduced into the model for fluid−solid interactions. The calculated equilibrium isotherm is in a good agreement with the desorption branch of the experimental isotherm on the reference 4.5 nm MCM-41 (Figure 3, left). In this comparison, the density of toluene in pores has been reduced by 6% to compensate for a higher bulk density in the model employed. Thus, the model provides a quantitative description of toluene adsorption on a reference material in a wide range of relative pressures.

In Figure 3 (right), we compare the experimental and MC simulated isotherms on micro-mesoporous PHTS material. Simulations were performed in a 7.3 nm diameter cylindrical pore. This value was determined from $N_2$ and Ar adsorption isotherms using the NLDFT equilibrium and metastable adsorption kernels[36] applied to the experimental desorption and adsorption branches, respectively. The mesopore and micropore volumes obtained from $N_2$ PSD are 0.49 cm$^3$/g and 0.15 cm$^3$/g, respectively. To account for the microporosity of PHTS, the simulated toluene isotherm was shifted upward by the amount adsorbed in micropores (∼1 mmol/g). The simulated toluene isotherm in Figure 3 (right) was converted into the adsorption isotherm reduced per unit weight using the mesopore volume of $V_{me} = 0.47$ cm$^3$/g and the micropore volume $V_{mi} = 0.1$ cm$^3$/g. The lower micropore volume obtained from toluene as compared to $N_2$ is most likely due to a molecular sieving effect. The adsorption branch of the GCMC isotherm exhibits capillary condensation transition between $P/P_0$ of ca. 0.53 and 0.55. GCMC desorption branch terminates at $P/P_0 = 0.08$. To calculate the equilibrium transition pressure, the gauge cell MC simulations[30] were performed, and the obtained S-shape isotherm (Figure 3, right) was integrated according to the Maxwell rule. The obtained equilibrium pressure of $P/P_0 = 0.42$ is in good agreement with the position of the experimental desorption step. It is worth noticing that the simulation in 7.3 nm pore is a prediction, and the fact the results are in agreement with experimental data indicates the consistency of our approach.

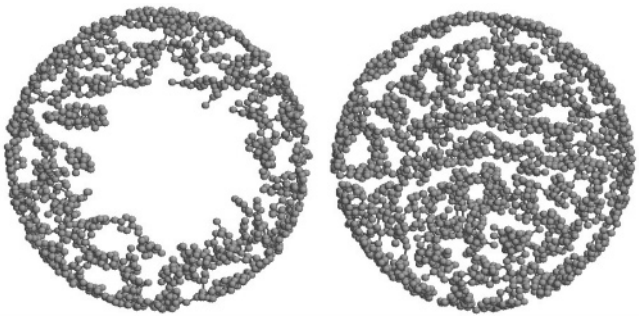

**Figure 2.** Snapshots from toluene adsorption simulations in a 4.5 nm MCM-41 pore before (left) and after (right) capillary condensation.

Gauge cell MC simulations also give the pressures of the vaporlike and liquidlike spinodals. Comparison with the experiment indicates that toluene adsorption in 7.3 nm pore corresponds to the regime of the developing hysteresis,[10] where capillary condensation occurs by nucleation, prior to reaching the spinodal limit. Earlier calculations of $N_2$ and Ar hysteresis loops in ∼7 nm cylindrical pores[10] indicated the regime of the developed

(34) Vishnyakov, A.; Neimark, A. V. *Langmuir* **2003**, *19*, 3240−3247.
(35) Yim, J. H.; Seon, J. B.; Jeong, T. D.; Pu, L. Y. S.; Baklanov, M. R.; Gidley, D. W. *Adv. Funct. Mater.* **2004**, *14*, 277−282.
(36) Neimark, A. V.; Ravikovitch, P. I. *Microporous Mesoporous Mater.* **2001**, *44*, 697−707.

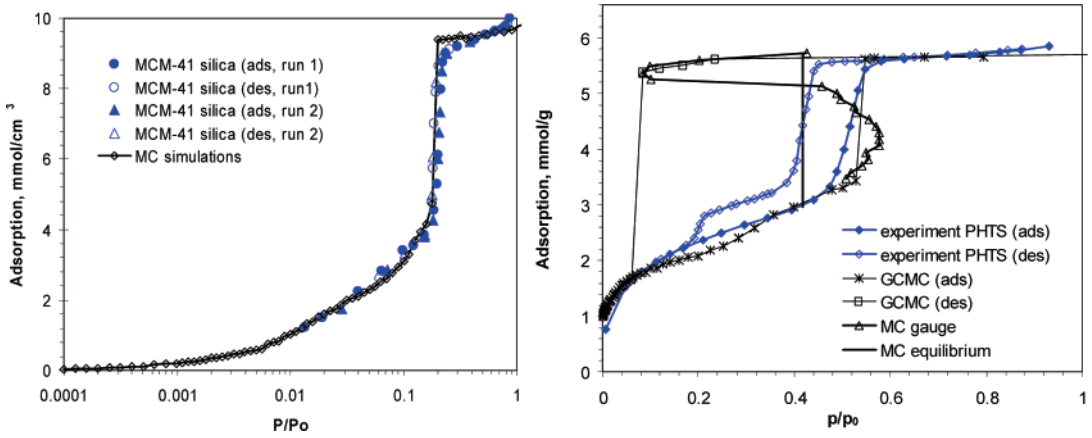


**Figure 3.** Left: Experimental and simulated equilibrium adsorption isotherm of toluene on 4.5 nm MCM-41 at 298 K. Right: Experimental isotherm of toluene on PHTS material at 298 K and simulated GCMC and gauge cell MC isotherms in a 7.3 nm cylindrical pore. Simulated isotherms are shifted upward by the amount adsorbed in PHTS micropores (∼1 mmol/g). See text.

hysteresis, where the capillary condensation occurs closer to the vaporlike spinodal. The difference between toluene and $N_2$/Ar is, probably, because of the difference in the nucleation energy barriers between simple gases and toluene, and it warrants further study. At the liquidlike spinodal limit, both simulations of toluene and NLDFT calculations for $N_2$ predict lower liquidlike spinodal pressure than the experimentally observed cavitation pressure.

**Macroscopic Model and Pore Size Distribution Calculations.** Using the molecular model developed, we generated equilibrium adsorption isotherms of toluene in 29 cylindrical pores ranging from 0.7 to 4.5 nm in diameter.[37] The isotherms are qualitatively similar to the isotherm on reference MCM-41 (Figure 3, left) and feature pore-filling steps that gradually shift to lower pressures as the pore diameter decreases. In pores wider than 4.5 nm, the simulations become expensive, and the theoretical isotherms were calculated by the augmented Derjaguin-Broekhoff-de Boer (DBdB) equations, which account for the fluid-solid interactions in terms of the disjoining pressure. The details are given in the Supporting Information. To avoid an ambiguity in the choice of the disjoining pressure isotherm due to a prominent sensitivity of toluene adsorption to the nature of silica surface,[38] we used the multilayer part of the isotherm on reference MCM-41. This isotherm was fitted to the exponential form.[38] We checked that the DBdB macroscopic approach provides a reasonably good description of the MC simulated isotherm in 7.3 nm pore, including equilibrium and vaporlike spinodal pressures.

The PSDs were calculated from the generalized adsorption integral (GAI) equation, which represents the experimental isotherm as a weighted sum of the theoretical isotherms in pores of different diameters.[39,40] Good agreement was obtained between the pore sizes assessed by $N_2$ and toluene adsorption (Table 1). Pore volumes obtained by toluene were ca. 3−9% lower than the nitrogen pore volumes, that can be attributed to the molecular sieving effect and some roughness of the pore surfaces. It should be noted that an earlier comparison showed that the effective pore volumes of MCM-41 materials probed by organic adsorptives (neopentane, *n*-hexane, benzene and methanol) are slightly lower than the values obtained by using $N_2$.[8]

## Conclusions

Comparison of nitrogen and toluene adsorption isotherms on ordered MCM-41 and PHTS materials demonstrates the universal features of capillary condensation of gases and organic vapors. It confirms that in uniform open cylindrical pores the desorption branch of the isotherm is close to the equilibrium transition. We developed a molecular model of toluene adsorption in silica nanopores that accounts for surface heterogeneity. The model parameters were fitted to reproduce the experimental isotherm on a reference 4.5 nm MCM-41. The model was then used to predict the hysteretic adsorption isotherm in a wider 7.3 nm PHTS material. A good agreement with experiment was found. We developed a hybrid method for PSD calculations from toluene adsorption isotherms that bridges molecular simulations and macroscopic equations. The PSDs obtained from toluene adsorption were consistent with the results of $N_2$ and Ar porosimetry. The developed method for calculating PSD from toluene adsorption has been recently applied to characterization of porous low-k dielectric films.[37]

**Acknowledgment.** This work was supported, in parts, by the International SEMATECH, the TRI/Princeton exploratory research program, the Fundação para a Ciência e Tecnologia, and the FEDER. We thank E. Van Bavel and P. Van der Voort (U. Antwerpen) for providing reference PHTS materials and M.R. Baklanov (IMEC) and C. Soles (NIST) for fruitful discussions.

**Supporting Information Available:** Detailed description of the models and parameters for toluene adsorption. This material is available free of charge via the Internet at http://pubs.acs.org.

LA052202K

(37) Ravikovitch, P. I.; Vishnyakov, A.; Neimark, A. V.; Ribeiro Carrott, M. M. L.; Russo, P. A.; Carrott, P. J. M. *AIP Conference Proceedings 788. Characterization and Metrology for ULSI Technology*; AIP: Woodbury, NY, 2005; pp 517−521.

(38) Schlangen, L. J. M.; Koopal, L. K.; Stuart, M. A. C.; Lyklema, J.; Robin, M.; Toulhoat, H. *Langmuir* **1995**, *11*, 1701−1710.

(39) Lawson, C. L.; Hanson, R. J. *Solving Least Squares Problems*; SIAM: Philadelphia, 1995.

(40) Ravikovitch, P. I.; Vishnyakov, A.; Russo, R.; Neimark, A. V. *Langmuir* **2000**, *16*, 2311−2320.